

More than meets the eye: magnetars in disguise

Wynn C. G. Ho,^{1*}

¹*School of Mathematics, University of Southampton, Southampton, SO17 1BJ*

Accepted 2012 October 30. Received 2012 October 4; in original form 2012 August 1

ABSTRACT

It has recently been proposed that radio emission from magnetars can be evaluated using a “fundamental plane” in parameter space between pulsar voltage gap and ratio of X-ray luminosity L_x to rotational energy loss rate \dot{E} . In particular, radio emission from magnetars will occur if $L_x/\dot{E} < 1$ and the voltage gap is large, and there is no radio emission if $L_x/\dot{E} > 1$. Here we clarify several issues regarding this fundamental plane, including demonstrating that the fundamental plane is not uniquely defined. We also show that, if magnetars and all other pulsars are different manifestations of a unified picture of neutron stars, then pulsar radio activity (inactivity) appears to be determined by the ratio $L_x/\dot{E} \lesssim 1$ ($L_x/\dot{E} \gtrsim 1$), although observational bias and uncertainty in the ratio for some sources may still invalidate this conclusion. Finally, we comment on the use of other pulsar parameters that are constructed from the three observables: spin period P , period derivative \dot{P} , and L_x .

Key words: pulsars: general — stars: magnetars — stars: neutron — X-rays: stars

1 INTRODUCTION

Anomalous X-ray pulsars (AXPs) and soft gamma-ray repeaters (SGRs) form the magnetar class of neutron stars, i.e., neutron stars which possess superstrong magnetic fields ($B \gtrsim 10^{14}$ G) in most cases. Their strong fields likely power the activity seen in these objects (see Woods & Thompson 2006; Mereghetti 2008, for review; see McGill SGR/AXP Online Catalog¹ for observational details). Two notable (and formerly defining) properties of magnetars are their high (as compared to that of other neutron stars of a similar age) observed X-ray luminosities L_x in quiescence and their non-detection at radio wavelengths. The first suggests that heat generated from the decay of a strong magnetic field is the source of their bright X-ray luminosity (Thompson & Duncan 1996; Heyl & Kulkarni 1998; Colpi et al. 2000; Aguilera et al. 2008) since L_x is greater than that available from their rotational and thermal reservoirs. The second suggests that magnetars do not emit in radio. However, recent observations have brought these characteristics into question, in particular, the discovery of X-ray luminosities lower than spin-down luminosities (or rate of rotational energy loss \dot{E}) for, and radio emission from, several magnetars (see Rea et al. 2012a, and references therein). The blurring of distinctions between magnetars and normal rotation-powered pulsars suggests magnetars may simply be a different manifestation of normal pulsars (see, e.g., Kaspi

2010; Perna & Pons 2011; Pons & Perna 2011), although radio emission from magnetars do show some behavior that are different than radio emission from normal pulsars (see discussion in Sec. 2 of Rea et al. 2012a, and references therein).

In light of these latest discoveries, Rea et al. (2012a) examine the observed properties of radio active and inactive magnetars. They notice that all radio magnetars have X-ray efficiency $L_x/\dot{E} < 1$. They also calculate the electric potential difference across the magnetic pole $\Delta\Phi$ (or voltage gap) for magnetars and normal pulsars and find an apparent anti-correlation between voltage gap and X-ray efficiency for magnetars. They then conduct simulations which can produce an anti-correlation between $\Delta\Phi$ and L_x/\dot{E} , depending on the neutron star magnetic field at birth. They conclude that there exists a fundamental plane ($\Delta\Phi$ versus L_x/\dot{E}) for radio magnetars, in which a magnetar will be radio active if $L_x/\dot{E} < 1$ and the voltage gap is large and radio inactive if $L_x/\dot{E} > 1$.

Here we point out that one needs to be careful about claiming trends and correlations between parameters (e.g., $\Delta\Phi$ and L_x/\dot{E}) when, in fact, these parameters are not entirely independent. We also extend the analysis of Rea et al. (2012a) by considering magnetars and other X-ray bright pulsars within the unified picture of neutron stars, as outlined in Kaspi (2010).

In Section 2, we briefly describe the standard model for pulsars and some of the basic equations derived from this model, as well as mention relevant recent works. In Section 3, we show results from using these equations and the observed

* Email: wynnho@slac.stanford.edu

¹ <http://www.physics.mcgill.ca/~pulsar/magnetar/main.html>

properties of magnetars and other pulsars. We summarize our results and discuss their implications in Section 4.

2 BASIC EQUATIONS OF PULSAR STANDARD MODEL

For rotation-powered pulsars, the conventional picture is that a pulsar emits radiation at a cost to its rotational energy, and the rate at which its rotational energy decreases is given by²

$$\dot{E} = 4\pi^2 I \frac{\dot{P}}{P^3} = \frac{2\pi^2 I}{P^2 \tau_c} = 4.0 \times 10^{46} \text{ ergs s}^{-1} I_{45} \frac{\dot{P}}{P^3}, \quad (1)$$

where I is the neutron star moment of inertia, P and \dot{P} are the spin period and spin period derivative, respectively, and $I_{45} = I/10^{45} \text{ g cm}^2$. The characteristic age of the pulsar (often used as an estimate of true age) is defined to be

$$\tau_c = \frac{P}{2\dot{P}}. \quad (2)$$

Note that equations (1) and (2) do not depend on a specific emission mechanism.

By assuming that the rotational energy is lost through magnetic dipole radiation, the pulsar magnetic field B can be inferred from observables P and \dot{P} , i.e.,

$$P\dot{P} = (\gamma/2)B^2 \Leftrightarrow B \sim 6.4 \times 10^{19} \text{ G } (P\dot{P})^{1/2}, \quad (3)$$

where $\gamma = 4\pi^2 R^6 \sin^2 \alpha / 3c^3 I = 4.884 \times 10^{-40} \text{ s G}^{-2} R_6^6 I_{45}^{-1} \sin^2 \alpha$, R is the neutron star radius, α is the angle between the stellar rotation and magnetic axes, and $R_6 = R/10^6 \text{ cm}$ (Gunn & Ostriker 1969). For radio emission, what is likely to be important is the electric potential difference across the magnetic pole, the maximum of which is approximately given by³ (Goldreich & Julian 1969)

$$\begin{aligned} \Delta\Phi &= \frac{BR}{2} \left(\frac{2\pi R}{cP} \right)^2 = \left(\frac{3\dot{E}}{2c \sin^2 \alpha} \right)^{1/2} \sim (3\dot{E}/2c)^{1/2} \\ &= 1.4 \times 10^{18} \text{ statvolts } (\dot{P}/P^3)^{1/2}. \end{aligned} \quad (4)$$

Clearly this voltage gap is trivially related to the rotational energy loss, i.e., $\Delta\Phi^2 \propto \dot{E}$. Therefore measuring \dot{E} is equivalent to determining $\Delta\Phi$ in the standard model for pulsar radio emission. In the following, we will only consider \dot{E} since it is a more fundamental parameter (i.e., it is derived from only I and two observables P and \dot{P}).

We note that the standard model described above follows from the early works of, e.g., Goldreich & Julian (1969); Ruderman & Sutherland (1975); Arons & Scharlemann (1979). More recently, the numerical calculations of pulsar magnetospheres by Spitkovsky (2006) find a modified equation for the energy emitted by an inclined, rotating neutron star. This leads to an inferred magnetic field at the magnetic equator [c.f. eq. (3), at the magnetic pole]

² There is a typo in the numerical value for rotational energy loss given in Rea et al. (2012a).

³ Eq. (2) of Rea et al. (2012a) gives the potential difference in statvolts; however the numerical value is actually in volts; similarly, the y -axes in both panels of Fig. 2 of Rea et al. (2012a) are in volts, not statvolts.

$$B \approx 2.6 \times 10^{19} \text{ G } [P\dot{P}/(1 + \sin^2 \alpha)]^{1/2} \quad (5)$$

and a voltage gap $\Delta\Phi \approx \{\dot{E}/[c(1 + \sin^2 \alpha)]\}^{1/2}$ [c.f. eq. (4)]. Furthermore, recent theoretical studies of the magnetosphere indicate that magnetar radio activity originates from closed magnetic field lines, in contrast to normal pulsar radio activity, and this difference could contribute to their differing observed properties; they also find the actual voltage gap to be much lower than that given by eq. (4), in particular $\Delta\Phi \sim 10^3 m_e c^2 \sim 10^6$ statvolts (see, e.g., Beloborodov & Thompson 2007; Beloborodov 2012; see also discussion in Sec. 4 of Rea et al. 2012a, and references therein).

3 COMPARISON TO OBSERVATIONS

We gather pulsar periods, period derivatives, spin-down luminosities, characteristic ages, and X-ray luminosities from the following: For rotation-powered radio pulsars, values for \dot{E} , τ_c , and L_x are taken from Becker (2009). For magnetars, values for \dot{E} and τ_c are taken from the McGill SGR/AXP Online Catalog. For all other sources, values for \dot{E} and τ_c are calculated from P and \dot{P} , which are obtained from the ATNF Pulsar Catalogue (Manchester et al. 2005)⁴, except in the case of 1E 1207.4–5209, where we consider two values of \dot{E} since there are two measured values of \dot{P} (Halpern & Gotthelf 2011). For magnetars, values for L_x are taken from Durant & van Kerkwijk (2006); Gelfand & Gaensler (2007); Muno et al. (2007); Rea et al. (2007, 2009b, 2012b); Esposito et al. (2008); Bernardini et al. (2009); Halpern & Gotthelf (2010b); Anderson et al. (2012), as well as Kaminker et al. (2009); Ng & Kaspi (2011), and references therein. For high magnetic field pulsars (three of which are rotating radio transients; McLaughlin et al. 2006), L_x upper limits are taken from Ng & Kaspi (2011), while L_x is calculated from those with measured temperature T and radius R (see Zhu et al. 2011, and references therein). For the ROSAT isolated neutron stars, L_x is calculated using T and R that are taken from Kaplan & van Kerkwijk (2011) and Zhu et al. (2011), and references therein. For PSR J0726–2612, L_x is calculated using T and R that taken from Speagle et al. (2011). For the central compact objects, L_x upper limits (for emission from the entire stellar surface) are taken from De Luca et al. (2004); Gotthelf et al. (2010); Halpern & Gotthelf (2010a). Note that the X-ray luminosities are used for illustrative purposes only since they are not calculated consistently between sources, and some sources are variable and have large distance uncertainties⁵.

Figure 1 shows \dot{E} as a function of L_x for our sources of interest. Also indicated is the line $L_x = \dot{E}$. It is evident that most magnetars possess X-ray luminosities which are not powered by their rotation since $L_x > \dot{E}$; this is a

⁴ <http://www.atnf.csiro.au/research/pulsar/psrcat/>

⁵ For example, PSR J1718–3718 could have an X-ray luminosity as high as $5 \times 10^{33} \text{ ergs s}^{-1}$, which would give $L_x/\dot{E} \approx 3$, an order-of-magnitude larger than that calculated from nominal values (Zhu et al. 2011). Similarly, PSR J0726–2612 has $L_x = 1.5 \times 10^{32} \text{ ergs s}^{-1}$ at a (uncertain) distance of 1 kpc (Speagle et al. 2011); a distance of 1.4 kpc would give $L_x/\dot{E} > 1$.

well-known and previously defining property for magnetars. Figure 2 shows \dot{E} as a function of L_x/\dot{E} , which can be interpreted as the efficiency of converting rotational energy loss into X-ray emission. Rea et al. (2012a) refer to this figure as the “fundamental plane for radio magnetars,” although they use the electric potential difference $\Delta\Phi$ for the y -axis (see footnote 3). Our Fig. 2 is equivalent to the fundamental plane since $\log \dot{E} = 2 \log \Delta\Phi + \text{constant}$ [see eq. (4)]. However, by using \dot{E} , we see more clearly that the fundamental plane is merely a rotation of Fig. 1, obtained by dividing the x -axis (i.e., L_x) by the y -axis (i.e., \dot{E}); the most obvious evidence for this rotation is the line $L_x = \dot{E}$. Thus the plane (Fig. 2) containing \dot{E} (or $\Delta\Phi$) and L_x/\dot{E} is no more fundamental, and contains no additional information, than what is already present in Fig. 1. Nothing can be said about the actual pulsar voltage gap, except as inferred from rotational energy loss.

Rea et al. (2012a) draw attention to the fact that magnetars and high- B pulsars appear to lie in a relatively narrow band along the diagonal in Fig. 2, i.e., there is an anti-correlation between \dot{E} and L_x/\dot{E} for these sources. They perform magneto-thermal simulations (see Pons et al. 2009, for details) and find evolutionary tracks that cluster approximately along this diagonal when the stars are born with fields $> 5 \times 10^{13}$ G. Furthermore, they find that these neutron stars evolve quickly to $L_x/\dot{E} > 1$, and this rapid movement through parameter space explains the absence of magnetars in the upper left of Fig. 2. First, we demonstrate that the clustering along the diagonal is an illusion and due to the particular choice of axes. In Fig. 2, we plot two lines that approximately span the observed magnetar clustering. These two lines are simply L_x/\dot{E} as a function of \dot{E} for constant values of L_x ($= 10^{33}$ and 2.5×10^{35} ergs s^{-1}); they arise because we are plotting $\log \dot{E} = -\log \dot{E} + \text{constant}$. Thus, while the magnetic field is likely to be important in determining the X-ray brightness of a pulsar (see Sec. 1 and 4), one does not need detailed knowledge of the field to understand magnetars in the parameter space of \dot{E} and L_x .

We next consider the fact that, for the neutron stars of interest here, there are only three observables: spin period P , period derivative \dot{P} , and X-ray luminosity L_x , with the first two yielding \dot{E} [see eq. (1)]. Thus far, we have only discussed two parameters, \dot{E} and L_x . Along each dashed line of L_x/\dot{E} as a function of \dot{E} in Fig. 2, we indicate particular values of a third parameter, the characteristic age τ_c [see eq. (2)], for a typical magnetar spin period $P = 5$ s (magnetars have spin periods between 2.1 and 11.8 s). It is clear that we can obtain “evolutionary sequences,” although no evolution is actually taking place since P is constant while \dot{P} is changing along each sequence. The lack of magnetars in the upper left of Fig. 2 is the same dearth of sources seen at short characteristic ages in the traditional P versus \dot{P} diagram for pulsars. In Figure 3, we show plots of the three observables P , \dot{P} , and L_x , with the first two in the form of \dot{E} and τ_c . The point here is to illustrate that the top panel (\dot{E} - τ_c) encodes no additional information than what is contained in the P - \dot{P} diagram; instead of inhabiting the upper right in P - \dot{P} parameter space, magnetars are in the lower left in \dot{E} - τ_c because of their longer spin periods [recall $\dot{E} \propto P^{-3}$; see eq. (1)]. On the other hand, the bottom panel (L_x/\dot{E} - τ_c) has additional information because it uses an independent

observable, i.e., magnetars tend to be more X-ray luminous than normal pulsars and have $L_x > \dot{E}$ (see Sec. 1).

Let us now examine the radio *inactivity* criterion $L_x/\dot{E} > 1$ (i.e., a source which satisfies this condition will not emit in radio) in the unification picture of neutron stars (i.e., that the very different observed properties of rotation-powered pulsars, magnetars, and other neutron stars are the result of a few intrinsic parameters, e.g., age and magnetic field; Kaspi 2010). Note that Rea et al. (2012a) only claim this criterion to be true for magnetars. From Figs. 1-3, we see that all pulsars, not just magnetars, with a measured $L_x > \dot{E}$ have not been observed to emit at radio wavelengths (for ROSAT isolated neutron stars, see Kondratiev et al. 2009; for central compact objects, see, e.g., De Luca 2008; Halpern & Gotthelf 2010a, for review). However, there are several high- B radio pulsars which have X-ray luminosity limits that still could allow them to violate the radio inactivity condition, especially PSR J1847–0130 with $L_x/\dot{E} < 200$ and PSR J1814–1744 with $L_x/\dot{E} < 90$. The criterion $L_x/\dot{E} < 1$ for radio *activity* also appears to be valid for most pulsars, not just magnetars; note that Rea et al. (2012a) argue that the two magnetars with $L_x < \dot{E}$ and are not seen in radio are, in actuality, radio emitters but have factors which have thus far prevented their detection in radio. We caution though that we use nominal values of L_x obtained from the literature and that some of these are subject to large uncertainties due to, e.g., unknown source distance. In particular, the uncertainties in inferred X-ray luminosities for the two radio pulsars PSR J1718–3718 and PSR J0726–2612 allow each to have $L_x > \dot{E}$ (see footnote 5). Also L_x is the X-ray luminosity as measured by a distant observer. If X-ray luminosity is a primary determinant in pulsar radio activity/inactivity, it is possible that the non-redshifted luminosity (or temperature) at the neutron star surface should be the proper value to use. Finally, it is of course possible that some sources have radio beams that never cross our line-of-sight and thus have not been detected in radio.

4 DISCUSSION

We showed that using the two prime pulsar observables, spin period P and period derivative \dot{P} , to calculate the voltage gap $\Delta\Phi$, as derived from standard pulsar theory (Goldreich & Julian 1969), yields no new information beyond what can be inferred from the spin-down luminosity \dot{E} . As a consequence, the parameter space or plane spanning $\Delta\Phi$ and L_x/\dot{E} is a simple transformation of, and no more fundamental or optimal than, the plane spanning \dot{E} and L_x . We showed that trends (in $\Delta\Phi$ and L_x/\dot{E} parameter space) seen among sources can be easily understood from standard pulsar theory and do not require complex simulations for explanation. For example, the anti-correlation between $\Delta\Phi$ and L_x/\dot{E} is a deception due to their particular dependence on P and \dot{P} . Finally, we showed that a condition for pulsar radio activity/inactivity based on X-ray efficiency ($L_x/\dot{E} \sim 1$) seems to hold true in the unified picture of neutron stars, although there exists sufficient uncertainties for some sources that they could invalidate this conclusion. Thus the mechanism for pulsar radio emission appears to be similar among the different classes of neutron stars.

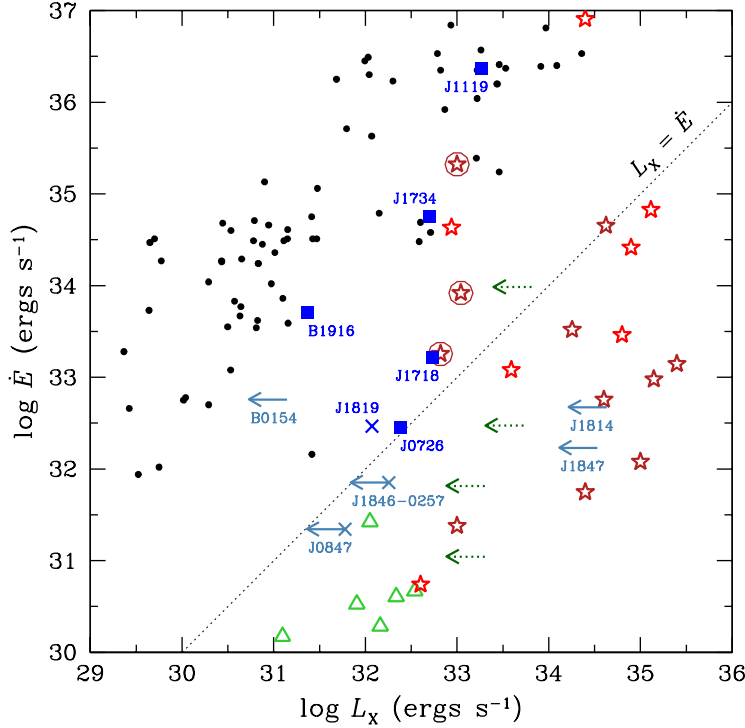


Figure 1. Rotational energy loss \dot{E} as a function of X-ray luminosity L_x . (Red) stars denote magnetars (AXPs/SGRs), and large circles around stars indicate magnetars that are detected in radio. (Blue) squares and labeled upper limits indicate high- B pulsars, while crosses indicate high- B pulsars which are rotating radio transients. (Green) triangles denote ROSAT isolated neutron stars, and dotted upper limits are for emission from the entire stellar surface of central compact objects. (Black) small circles denote rotation-powered radio pulsars. Dotted line indicates $L_x = \dot{E}$.

However there are important differences between the observed properties of radio emission from magnetars and normal pulsars (see Rea et al. 2012a, and references therein), and these are likely due in part to differences in emission location and magnetic field strength/geometry of the magnetosphere (see, e.g., Beloborodov & Thompson 2007; Beloborodov 2012, and references therein). New sources and improved measurements would provide a better understanding of radio behavior, as well as continuing theoretical work.

Up to this point, we have not discussed one other parameter, magnetic field B , that is often used to compare magnetars and pulsars. The most common method of determining B for individual sources is by using eq. (3) [or eq. (5); see also Glampedakis & Andersson 2011, where it is argued that using eq. (3) for magnetars leads to an overestimate of B]. In this case, our statements regarding comparisons between parameters that are only derived from the two observables P and \dot{P} apply here as well. For example, plots of B versus τ_c provide no additional information than what is contained within the standard pulsar P - \dot{P} diagram, while plots of surface temperature T versus B (see, e.g., Pons et al. 2007; Zhu et al. 2009) and T versus τ_c (see, e.g., Kaplan & van Kerkwijk 2011) are similar to L_x - \dot{E} (though there are systematic differences between measurements of T and L_x). On the other hand, independent measurements of magnetic field (from, e.g., spectral lines) or true ages (from, e.g., supernova remnants) do yield new information and are thus extremely valuable. In regards to the latter, we note

that, for young pulsars, characteristic age generally disagrees with true age in cases where both can be determined (see, e.g., Ho & Andersson 2012).

Finally, the reason why magnetars exhibit high X-ray luminosities L_x (for their age) is not known for certain. What is known is that an additional source of internal heat (beyond residual heat from neutron star formation) must be present in the outer crust (Kaminker et al. 2006, 2009; Ho et al. 2012). Magnetic field evolution and decay could provide this heat source (see, e.g., Pons et al. 2007, 2009; Cooper & Kaplan 2010; Price et al. 2012). We note that several magnetars may have very similar X-ray luminosities (see Fig. 1; see also Durant & van Kerkwijk 2006); this could suggest that their crustal field strengths are similar and the field decay timescale is longer than the age of the oldest of these sources.

ACKNOWLEDGMENTS

WCGH thanks Nils Andersson and the anonymous referee for comments and José Pons and Nanda Rea for discussion and clarifications. WCGH acknowledges support from the Science and Technology Facilities Council (STFC) in the UK.

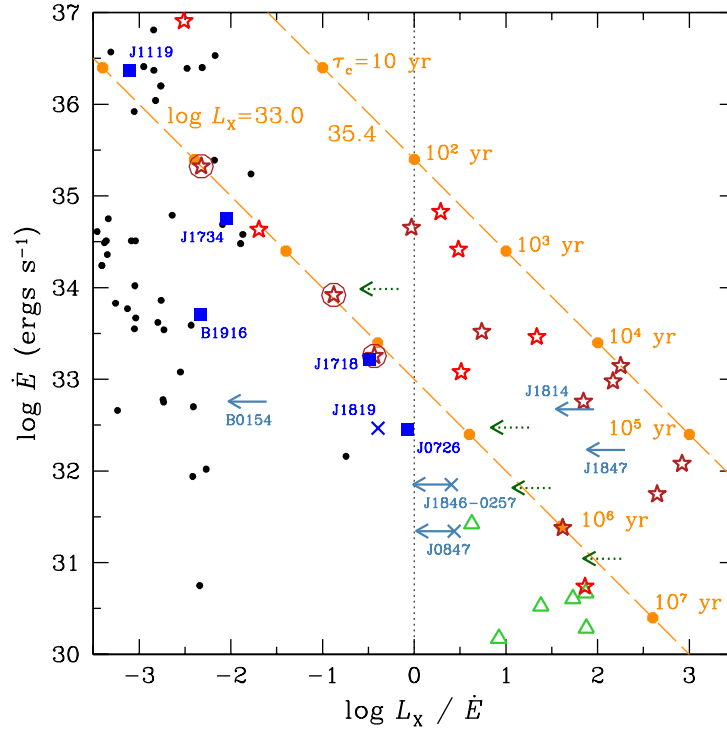


Figure 2. Rotational energy loss \dot{E} as a function of X-ray efficiency L_x/\dot{E} . (Red) stars denote magnetars (AXPs/SGRs), and large circles around stars indicate magnetars that are detected in radio. (Blue) squares and labeled upper limits indicate high- B pulsars, while crosses indicate high- B pulsars which are rotating radio transients. (Green) triangles denote ROSAT isolated neutron stars, and dotted upper limits are for emission from the entire stellar surface of central compact objects. (Black) small circles denote rotation-powered radio pulsars. Dotted line indicates $L_x/\dot{E} = 1$. Dashed lines indicate L_x/\dot{E} for $\log L_x = 33.0$ and 35.4 , and filled circles give the characteristic age τ_c (assuming $P = 5$ s).

REFERENCES

- Aguilera, D. N., Pons, J. A., & Miralles, J. A. 2008, *ApJ*, 673, L167
- Anderson, G. E., Gaensler, B. M., Slane, P. O. et al. 2012, *ApJ*, 751, 53
- Arons, J. & Scharlemann, E. T. 1979, *ApJ*, 231, 854
- Becker, W. 2009, in Becker W., eds, *Ap&SS Lib. Vol. 357, Neutron Stars and Pulsars*. Springer-Verlag, Berlin, p. 91
- Beloborodov, A. M. 2012, *ApJ*, submitted (arXiv:1209.4063)
- Beloborodov, A. M. & Thompson, C. 2007, *ApJ*, 657, 967
- Bernardini, F., Israel, G. L., Dall’Osso, S. et al. 2009, *A&A*, 498, L95
- Colpi, M., Geppert, U., & Page, D. 2000, *ApJ*, 529, L29
- Cooper, R. L. & Kaplan, D. L. 2010, *ApJ*, 708, L80
- De Luca, A. 2008, in Bassa C. G., Wang Z., Cumming A., Kaspi V. M., eds, *AIP Conf. Ser. 983: 40 Years of Pulsars*. AIP, Melville, NY, p. 311
- De Luca, A., Mereghetti, S., Caraveo, P. A., Moroni, M., Mignani, R. P., & Bignami, G. F. 2004, *A&A*, 418, 625
- Durant, M. & van Kerkwijk, M. H. 2006, *ApJ*, 650, 1070
- Esposito, P., Israel, G. L., Zane, S. et al. 2008, *MNRAS*, 390, L34
- Gelfand, J. D. & Gaensler, B. M. 2007, *ApJ*, 667, 1111
- Glampedakis, K. & Andersson, N. 2011, *ApJ*, 740, L35
- Goldreich, P. & Julian, W. H. 1969, *ApJ*, 157, 869
- Gotthelf, E. V., Perna, R., & Halpern, J. P. 2010, *ApJ*, 724, 1316
- Gunn, J. E. & Ostriker, J. P. 1969, *Nature*, 221, 454
- Halpern, J. P. & Gotthelf, E. V. 2010a, *ApJ*, 709, 436
- Halpern, J. P. & Gotthelf, E. V. 2010b, *ApJ*, 725, 1384
- Halpern, J. P. & Gotthelf, E. V. 2011, *ApJ*, 733, L28
- Heyl, J. S. & Kulkarni, S. R. 1998, *ApJ*, 506, L61
- Ho, W. C. G. & Andersson, N. 2012, *Nature Phys.*, in press (arXiv:1208.3201)
- Ho, W. C. G., Glampedakis, K., & Andersson, N. 2012, *MNRAS*, 422, 2632
- Kaminker, A. D., Yakovlev, D. G., Potekhin, A. Y., Shibasaki, N., Shternin, P. S., & Gnedin, O. Y. 2006, *MNRAS*, 371, 477
- Kaminker, A. D., Potekhin, A. Y., Yakovlev, D. G., & Chabrier, G. 2009, *MNRAS*, 395, 2257
- Kaplan, D. L. & van Kerkwijk, M. H. 2011, *ApJ*, 740, L30
- Kaspi, V. M. 2010, *Publ. Natl. Acad. Sci.*, 107, 7147
- Kondratiev, V. I., McLaughlin, M. A., Lorimer, D. R. et al. 2009, *ApJ*, 702, 692
- Manchester, R. N., Hobbs, G. B., Teoh, A., & Hobbs, M. 2005, *AJ*, 129, 1993
- McLaughlin, M. A., Lyne, A. G., Lorimer, D. R. et al. 2006, *Nature*, 439, 817
- Mereghetti, S. 2008, *A&A Rev.*, 15, 225
- Muno, M. P., Gaensler, B. M., Clark, J. S., de Grijs, R., Pooley, D., Stevens, I. R., & Portegies Zwart, S. F. 2007,

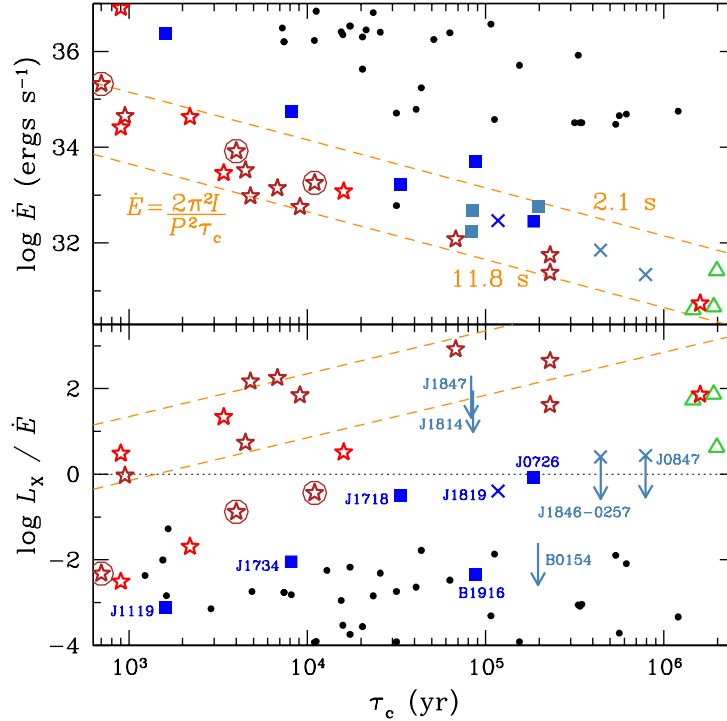


Figure 3. Rotational energy loss \dot{E} (top panel) and X-ray efficiency L_x/\dot{E} (bottom panel) as a function of characteristic age τ_c . (Red) stars denote magnetars (AXPs/SGRs), and large circles around stars indicate magnetars that are detected in radio. (Blue) squares and labeled upper limits indicate high- B pulsars, while crosses indicate high- B pulsars which are rotating radio transients. (Green) triangles denote ROSAT isolated neutron stars, and dotted upper limits are for emission from the entire stellar surface of central compact objects. (Black) small circles denote rotation-powered radio pulsars. Dotted line indicates $L_x/\dot{E} = 1$. Dashed lines indicate \dot{E} and L_x/\dot{E} (taking $L_x = 10^{35}$ ergs s $^{-1}$) for spin periods $P = 2.5$ s and 11.8 s, where $\dot{E} \propto 1/(P^2\tau_c)$ [see eq. (1)].

MNRAS, 378, L44

Ng, C.-Y. & Kaspi, V. M. 2011, in Göğüş E., Belloni T., Ertan Ü., eds, AIP Conf. Proc. 1379, Astrophysics of Neutron Stars 2010. AIP, Melville, NY, p. 60

Perna, R. & Pons, J. A. 2011, ApJ, 727, L51

Pons, J. A. & Perna, R. 2011, ApJ, 741, 123

Pons, J. A., Link, B., Miralles, J. A., & Geppert, U. 2007, Phys. Rev. Lett., 98, 071101

Pons, J. A., Miralles, J. A., & Geppert, U. 2009, A&A, 496, 207

Price, S., Link, B., Epstein, R. I., & Li, H. 2012, MNRAS, 420, 949

Rea, N., Nichelli, E., Israel, G. L., et al. 2007, MNRAS, 381, 293

Rea, N., McLaughlin, M. A., Gaensler, B. M. et al. 2009a, ApJ, 703, L41

Rea, N., Israel, G. L., Turolla, R. et al. 2009b, MNRAS, 396, 2419

Rea, N., Pons, J. A., Torres, D. F., & Turolla, R. 2012a, ApJ, 748, L12

Rea, N., Israel, G. L., Esposito, P. et al. 2012b, ApJ, 754, 27

Ruderman, M. A. & Sutherland, P. G. 1975, ApJ, 196, 51

Speagle, J. S., Kaplan, D. L., & van Kerkwijk, M. H. 2011, ApJ, 743, 183

Spitkovsky, A. 2006, ApJ, 648, L51

Thompson, C. & Duncan, R. C. 1996, ApJ, 473, 322

Woods, P. M. & Thompson, C. 2006, in Lewin, W. H. G., van der Klis, M., eds, Compact Stellar X-ray Sources. Cambridge University Press, Cambridge, p. 547

Zhu, W., Kaspi, V. M., Gonzalez, M. E., & Lyne, A. G. 2009, ApJ, 704, 1321

Zhu, W., Kaspi, V. M., McLaughlin, M. A., Pavlov, G. G., Ng, C.-Y., Manchester, R. N., Gaensler, B. M., & Woods, P. M. 2011, ApJ, 734, 44